10.1109/ULTSYM.2010.0567

Optimizing CMUT Geometry for High Power

F. Yalcin Yamaner[1], *Student Member, IEEE*, Selim Olcum[2], *Student Member, IEEE*, Ayhan Bozkurt[1], *Member, IEEE*, Hayrettin Köymen[2], *Senior Member, IEEE* and Abdullah Atalar[2], *Fellow, IEEE*

[1] Sabanci University, Electronics Engineering, Istanbul, Turkey
[2] Bilkent University, Electrical and Electronics Engineering Department, Ankara, Turkey

***Abstract*— Capacitive micromachined ultrasonic transducers (CMUTs) have demonstrated various advantages over piezoelectric transducers. However, current CMUT designs produce low output pressures with high harmonic distortions. Optimizing the transducer parameters requires an iterative solution and is too time consuming using finite element (FEM) modelling tools. In this work, we present a method of designing high output pressure CMUTs with relatively low distortion. We analyze the behavior of a membrane under high voltage continuous wave operation using a nonlinear electrical circuit model. The radiation impedance of an array of CMUTs is accurately represented using an RLC circuit in the model. The maximum membrane swing without collapse is targeted in the transmit mode. Using SPICE simulation of the parametric circuit model, we design the CMUT cell with optimized parameters such as the membrane radius (a), thickness (t_m), insulator thickness (t_i) and gap height (t_g). The model also predicts the amount of second harmonic at the output. To verify the accuracy of the results, we built a FEM model with the same CMUT parameters. The design starts by choosing t_i for the given input voltage level. First, a is selected for the maximum radiation resistance of the array at the operating frequency. Second, t_m is found for the resonance at the input frequency. Third, t_g is chosen for the maximum membrane swing. Under this condition, a frequency shift in the resonant frequency occurs. Second and third steps are repeated until convergence. This method results in a CMUT array with a high output power and with low distortion.**

I. Introduction

High intensity focused ultrasound (HIFU) is a state of the art treatment technique of cancers. Treatment is done by destruction of the abnormal tissue using high energy, high frequency focused sound waves. HIFU tools have been in use for the last 50 years, and since the introduction of the technology, piezoelectric transducers have been the core element of the device. Recently, it has been demonstrated that CMUTs are strong competitors and can be used as a HIFU transducer [1]. As CMUTs are fabricated using silicon micromachining techniques, it is possible to design a CMUT that operates at a specific frequency. The main drawback of present CMUT designs is the lack of efficiency in the output pressure. Due to the nonlinearity of the CMUT, the optimization must be done considering the harmonic distortions caused by continuous wave operation. Such an optimization takes too much time using current finite element simulation tools [2]. In this work, we analyzed the uncollapsed behaviour of a CMUT over a proposed nonlinear electrical circuit model and the steps followed are shown for the optimization of the CMUT parameters. The proposed model can be used to optimize a CMUT array to obtain a high output power with low distortion required for a high power operation.

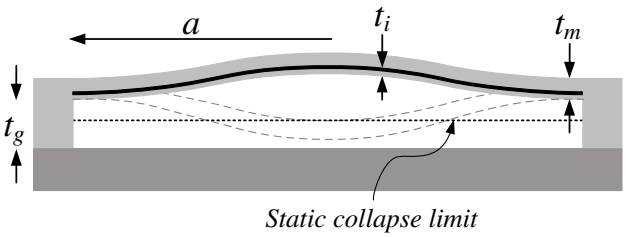

Fig. 1. Cross section of a circular membrane with radius a, thickness t_m and gap height of t_g. The top electrode is at a distance t_i above from the gap. The substrate is used as a bottom electrode.

II. Nonlinear Electrical Circuit Model of a CMUT

The behavior of a CMUT under high voltage continuous wave operation is simulated using a nonlinear electrical circuit model. The model predicts the uncollapsed mechanical movement of a CMUT for an applied electrical signal. It also enables the analysis and optimization of CMUT parameters for the given operation conditions.

A. CMUT Parameters

The Fig. 1 shows the cross section of a circular CMUT cell modeled in this work. We assume that the electrodes have a full coverage over the membrane region. The bottom electrode is the conductive substrate itself. The key parameters are membrane radius a, membrane thickness t_m, insulating layer thickness t_i and gap height t_g. The material properties of the membrane are given in Table I.

Young modulus, Y_0	3.2e11
Permittivity, ϵ_m	7.5
Density, ρ	3270
Poisson Ratio, σ	0.263

TABLE I
Membrane Material Properties

We define an effective gap parameter, t_{ge} as

$$t_{ge} = t_g + \frac{t_i}{\epsilon_m} \tag{1}$$

where ϵ_m is is the permittivity of the membrane material.

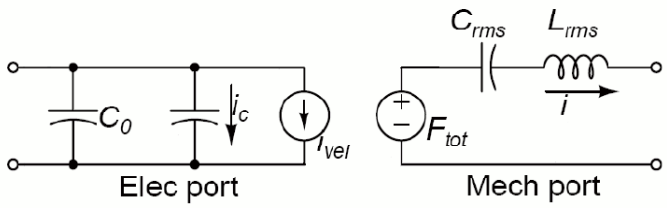

Fig. 2. The nonlinear equivalent circuit model of a CMUT.

B. CMUT Model

The proposed circuit model of CMUT consists of two ports as shown in Fig. 2. We preferred the root mean square (rms) velocity instead of the average velocity as the lumped through variable. C_0 in the electrical port represents the undeflected capacitance of the transducer. The second capacitor in the same port represents the additional capacitance due to deflection. i_{vel} is the current generated by the mechanical movement. The mechanical side is modeled using lumped parameters. The membrane mass is represented by an inductance (L_{rms}) with a value

$$L_{rms} = \rho t_m \pi a^2 \tag{2}$$

and the inverse of the spring constant is modelled by a capacitance (C_{rms}) of value

$$C_{rms} = 1.8 \left[\frac{16\pi Y_0 t_m^3}{(1-\sigma^2)a^2} \right]^{-1} \tag{3}$$

F_{tot} represents the total force acting on the membrane. The current in the mechanical side of the circuit represents the rms velocity v_{rms}. The charge on the capacitor C_{rms} is the rms displacement of the membrane. When this value is multiplied with $\sqrt{5}$, the peak displacement at the center of the membrane (x_p) is obtained. The nonlinear parameters in the model were previously [3] calculated as follows[1]

$$i_{vel} = \frac{C_0 V(t)}{2x_p(t)} \frac{x_p(t)}{dt} \left[\frac{t_{ge}}{t_{ge} - x_p(t)} - \frac{\tanh^{-1}(\sqrt{x_p(t)/t_{ge}})}{\sqrt{x_p(t)/t_{ge}}} \right] \tag{4}$$

$$F_{tot} = \frac{\sqrt{5} C_0 V^2(t)}{12 t_{ge}} \left[\frac{t_{ge}}{t_{ge} - x_p(t)} + \frac{\tanh^{-1}(\sqrt{x_p(t)/t_{ge}})}{\sqrt{x_p(t)/t_{ge}}} \right] \tag{5}$$

III. Modelling Nonlinear Components in SPICE

To simulate the nonlinear circuit model, LTSpice, a public domain SPICE simulator, is used. To model i_c and i_{vel}, "behavioral current source" is used. F_{tot} is modeled using a "behavioral voltage source". A small circuit is also created with a voltage controlled voltage source to generate the x_p value.

The model is checked to predict the static deflection under a static bias and the results are compared in Fig. 3. The model predicted x_p value accurately at lower voltages but it did not match FEM results at higher voltage levels. Consequently, a correction term is used to make the model more accurate.

[1]Missing $\sqrt{5}/3$ factor in F_{tot} of Ref. [3] is corrected here.

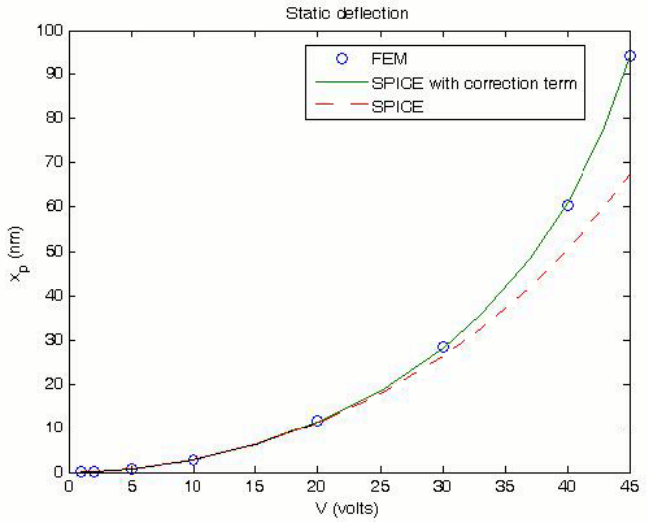

Fig. 3. The static deflection at the center of the membrane as calculated by FEM, the circuit model and the corrected circuit model.

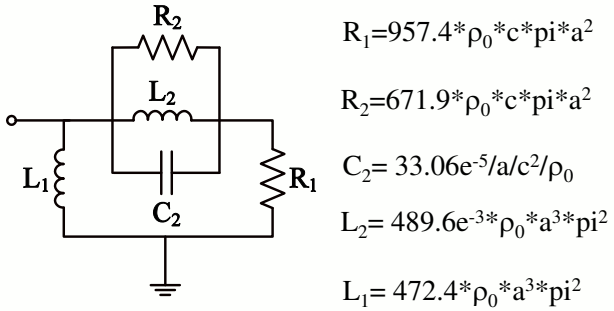

Fig. 4. The circuit model of the radiation impedance of a single CMUT cell.

A. Radiation Impedance

As the operation is done in liquid environment, the radiation impedance has to be modeled correctly and included in the mechanical side of the circuit model. It is important to note that the radiation impedance is frequency dependent and it is not purely real. It depends on the membrane profile, the number and positions of CMUT cells [4]. In this circuit model, we worked on two different element configurations: one with a single CMUT cell and the other with an array of seven CMUT cells.

1) Single CMUT Cell: The equivalent circuit model for the radiation impedance of a single CMUT cell is shown in Fig. 4. The inductor L_1 takes care of the zero impedance at $ka = 0$ (k is the wavenumber in the immersion medium) and the resistor R_1 models the finite resistance at $ka = \infty$. The other circuit components R_2, L_2, and C_2 model the impedance peak at $ka = 4$. The resulting circuit predicts the radiation impedance of a single CMUT cell very accurately (Fig. 5).

2) Array of seven CMUT Cells: The radiation impedance of an array of CMUT cells is more complex. Each cell has a different radiation resistance depending on the position in

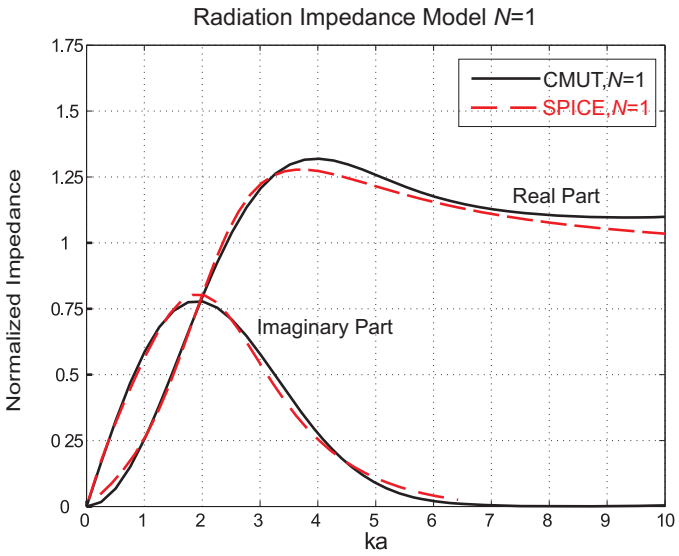

Fig. 5. The modelled radiation impedance of a single CMUT cell as a function of ka.

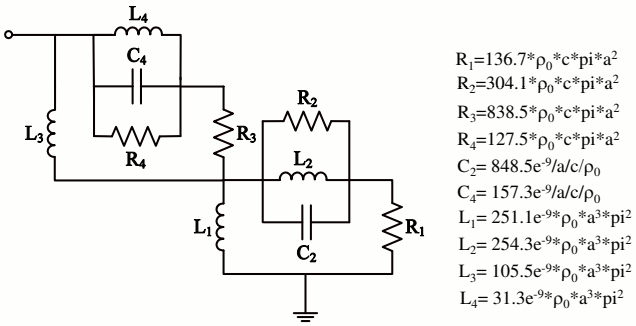

Fig. 6. The circuit model of the radiation impedance of an array of seven CMUT cells.

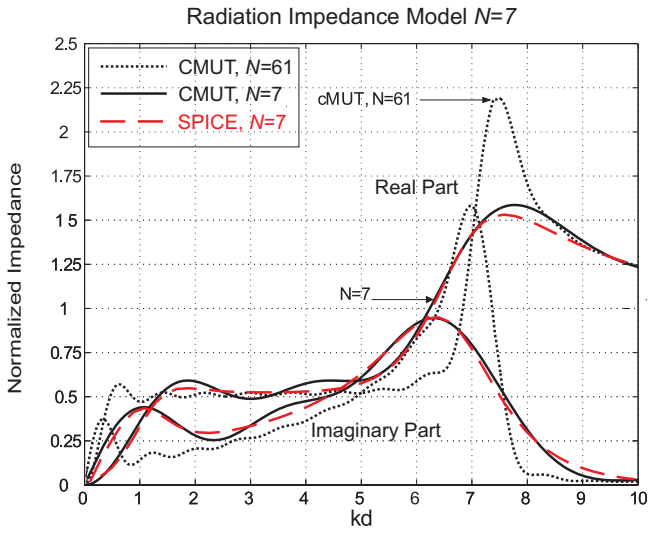

Fig. 7. The modelled radiation impedance of an array of seven CMUT cells (d=2a, where d is the center to center distance of cells).

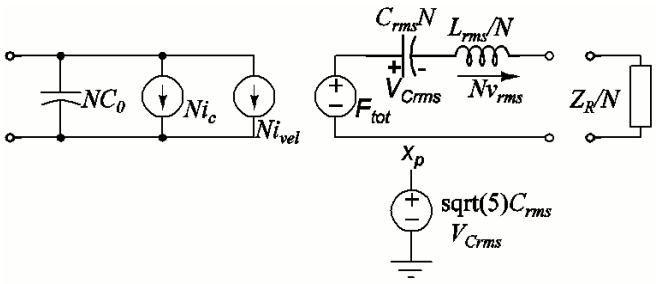

Fig. 8. The equivalent circuit model of an array of N CMUT cells.

the array and there are mutual impedances between array elements. To simplify this complex model, we define a "representative radiation impedance to approximate the average behavior of the array. Fig. 6 shows the radiation resistance model of an array of seven CMUT cells. The components R_4, L_4 and C_4 model the impedance peak at $ka = 7.5$. The behavior of this circuit is given in the Fig. 7.

The equivalent circuit model of CMUT for a N cell array is shown in Fig. 8 including the complex radiation impedance Z_R.

IV. Optimization of CMUT Parameters

Suppose our main goal is to get maximum membrane swing at the frequency of the operation without collapse. We find the optimum parameters of the membrane using the electrical circuit model. The procedure starts by choosing a safe t_i value to allow for the maximum input voltage, since t_i value determines the breakdown voltage. Then the radius a is selected for the maximum radiation resistance of the array at the operating frequency. Since the radiation resistance peak is at ka=3.5, a is chosen accordingly. The second step is to find t_m for a resonance of the membrane at the operating frequency. The last step is for enabling the maximum swing at the given excitation voltage by minimizing t_g in such a way that no collapse occurs. After this step, a frequency shift occurs in the resonant frequency. To equate the resonance frequency with the operating frequency, the second and third steps are repeated iteratively.

V. Results

The first optimization is done for a single CMUT at 5 MHz. The available maximum drive voltage is assumed to be 100V. Thus, the insulating thickness t_i is chosen as 200 nm for a safe operation. The radius of the membrane is chosen as 183μm to obtain the maximum radiation resistance at this frequency. Using the proposed model the membrane thickness and the gap are optimized for a full membrane swing. The resulting membrane thickness and the gap are found to be 44μm and 95nm, respectively. The resulting center displacement is compared with the FEM as shown in Fig. 9. As seen from the figure membrane swings the whole gap without touching the bottom surface and even moves 40nm above its initial position. The corresponding pressure is given in Fig. 10. To check the second harmonic, the fourier transform of the output pressure signal is plotted (Fig. 11). The second harmonic in the output pressure of the optimized CMUT cell is found 20dB less than the the fundamental. The equivalent circuit model performs a simulations within seconds, on the other hand FEM

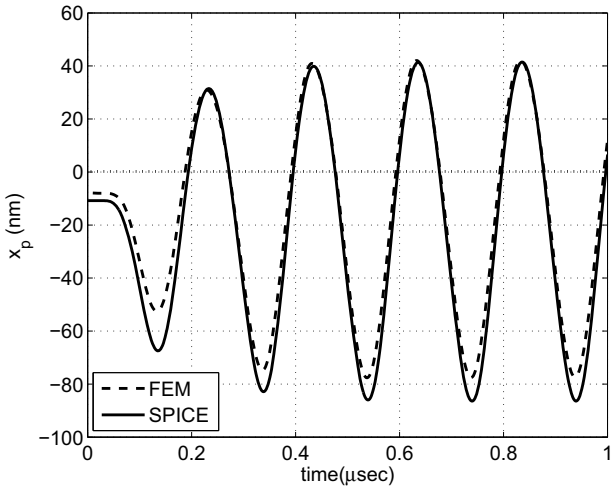

Fig. 9. Comparison of the center displacement for a 100V$_{p-p}$ burst 5 MHz input signal.

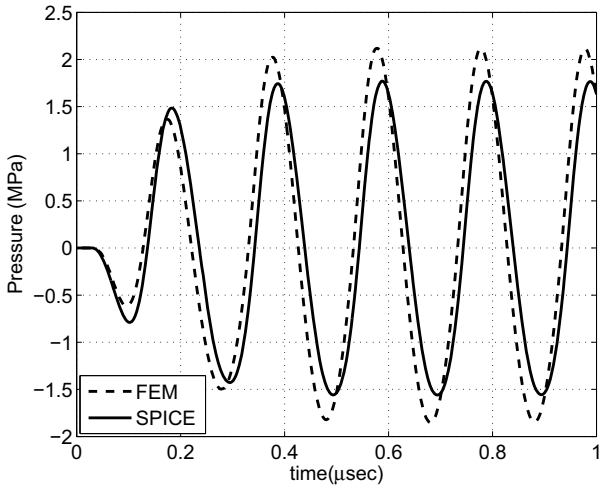

Fig. 10. Comparison of the surface pressure for a 100V$_{p-p}$ burst 5 MHz input signal.

simulations takes around 30 minutes. The model and FEM results matches with an error of 5%.

The second optimization is done for an array of 7 CMUT cells. The parameters of the different designs and the results are given at the Table II. All membranes are chosen to resonate at 5 MHz. The highest power density is obtained when the membrane is relatively thick (41.5μm) and the radius is large (183μm). By this optimization, we get about 20% improvement in pressure, 40% improvement in power. Moreover, the second harmonic is reduced by about 10dB.

VI. Conclusions

The proposed model can be used to optimize CMUTs effectively. For a high power CMUT operation, the cMUT cell radius should be chosen to maximize the radiation resistance at the operating frequency. Membrane thickness should be chosen to resonate at the operating frequency and gap should be chosen to give full swing at the given applied voltage.

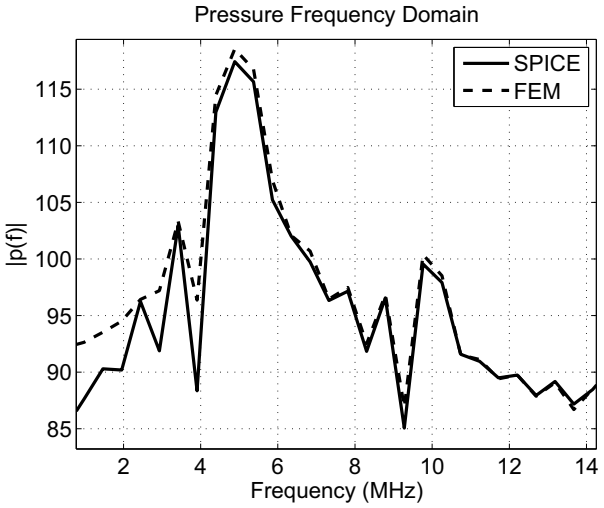

Fig. 11. Comparison of the pressure frequency spectrum for a 100V$_{p-p}$ burst 5 MHz input signal.

a	t_m	t_g	x_p	Pres.	Harmon.	Power Dens.
(μm)	(μm)	(nm)	(nm p-p)	(MPa)	(dB)	(W/mm^2)
20	1.17	168	224	0.852	-12	0.486
40	3.5	135.5	167	0.860	-8	0.493
60	6.1	135	182	0.952	-13	0.605
90	11.6	128	188	0.981	-15	0.645
183	41.5	83	121	1.084	-18	0.783
214	48	81	121	1.033	-27	0.712

TABLE II
Design Comparisons at 5 MHz. (100V$_{p-p}$, t_i =200nm, N=7)

As a future work, a fabrication will be done with the optimized CMUT parameters and experiments will be done on the fabricated CMUTs to verify the results.

Acknowledgements

This work was supported by TUBITAK under project grants 104E067, 105E023 and 107T921. S.O. gratefully acknowledge the financial support of TUBITAK and ASELSAN A.Ş. for their Graduate Scholarship and Ph.D. Fellowship Programs. A.A. acknowledges the support of TUBA.

References

[1] S. H. Wong, R. D. Watkins, M. Kupnik, K. B. Pauly, and B. T. Khuri-Yakub, "Feasibility of MR-temperature mapping of ultrasonic heating from a CMUT," *IEEE Trans. Ultrason., Ferroelect., Freq. Contr.*, vol. 55, pp. 811–818, 2008.

[2] A. Lohfink and P. C. Eccardt, "Linear and nonlinear equivalent circuit modeling of CMUTs," *IEEE Trans. Ultrason., Ferroelect., Freq. Contr.*, vol. 52, pp. 2163–2172, 2005.

[3] H. K. Oguz, S. Olcum, M. N. Senlik, V. Tas, A. Atalar, and H. Köymen, "Nonlinear modeling of an immersed transmitting capacitive micromachined ultrasonic transducer for harmonic balance analysis," *IEEE Trans. Ultrason., Ferroelect., Freq. Contr.*, vol. 57, pp. 438–447, 2010.

[4] M. N. Senlik, S. Olcum, H. Köymen, and A. Atalar, "Radiation impedance of an array of circular capacitive micromachined ultrasonic transducers," *IEEE Trans. Ultrason., Ferroelect., Freq. Contr.*, vol. 57, pp. 969–976, 2010.